Amorphous water ice and its ability to trap gases

A. Bar-Nun, J. Dror, E. Kochavi, and D. Laufer
Department of Geophysics and Planetary Sciences, Tel Aviv University, Ramat Aviv, 69 978 Tel Aviv, Israel
(Received 1 April 1986; revised manuscript received 19 September 1986)

The trapping of argon by amorphous water ice at 19—80 K and its release from the ice were studied experimentally, by flowing gas into ice, or by codepositing a gas-water vapor mixture. Upon warming the gas-laden ice, the trapped argon is released from it in seven temperature ranges: (a) 23 K, (b) 35 K, (c) 44 K, (d) ~80 K, (e) 136.8 K, (f) 160.0 K, and (g) ~180 K. The amount of internally trapped argon, in (b)—(g), can be as high as 3.3 times the amount of the ice itself. By using argon to probe the ice's structure and dynamics, it was found that the highly porous amorphous ice anneals at all temperatures, at a rate which is strongly temperature dependent, and transforms into the cubic form at 136.8±1.6 K and then into the hexagonal form at 160.0±1.0 K. When gas is made to flow into the amorphous ice, it fills open holes and cracks in it with gaseous or frozen argon, depending upon the temperature. The slow creeping of the ice closes some gas-filled holes and squeezes out some of the gas, while locking the rest and letting it escape only during the transformations. The last range, (g), is attributed to the simultaneous evaporation of gas and water from the argon clathrate-hydrate. Gas flow at a pressure exceeding 2.6 dyn cm^{-2}, results in a very fluffy ice, with a density of only 0.17 g cm^{-3}. The release of gas from this kind of ice, or from ice codeposited with gas, is accompanied by massive ejection of 0.1—1-μm ice grains and by argon jets, which propel them. Many of the experimental findings could be important for interpreting observations on comets, icy satellites, icy ring particles, and interstellar grains.

I. INTRODUCTION

The realization that water ice is the major constituent of comets, the satellites of the outer planets and their rings particles, and of the icy grain mantles in dense interstellar clouds, prompted us to study in detail the properties of water ice at very low temperatures, with an emphasis on its ability to trap various gases. In a previous paper,[1] we reported the trapping of CO, CH_4, N_2, and Ar, by four different mechanisms, resulting in the release of each gas from the ice at four different temperature ranges: 30—60 K, where the gas frozen on the water ice surface evaporates; 135—155 K, where trapped gas is squeezed out of the ice during its transformation from amorphous into cubic ice; occasionally, at 160—175 K, where deeply buried gas is released during the transformation of cubic ice into hexagonal ice; and 165—190 K, where gas and water are released simultaneously, during the evaporation of a clathrate-hydrate. It was also found that the ratio of trapped gas to water ice could reach values considerably larger than 1:1. In addition, we reported the trapping of H_2 and CO_2 and the massive ejection of ice grains during gas evolution from the ice. The experimental findings enable us to propose some possible explanations to various observations on the behavior of comets and the composition of Titan's atmosphere.

Nevertheless, the very complex behavior of water ice, which was found in these experiments and in the experiments of Ghormly,[2] together with the yet unsettled questions regarding the possible existence of a glass transition and the exact temperatures at which amorphous ice transforms into cubic ice and then into hexagonal ice (e.g., Refs. 3 and 4), merited a further, much more detailed, study of the ice's structure and dynamics. Of special interest was the elucidation of the mechanisms by which gas is trapped in the ice in such a way that it comes out in so many temperature ranges. Argon, which does not react with water, was chosen as a probe for studying these processes.

II. EXPERIMENTAL

The experimental setup and procedures were described in detail in our previous papers[1,5] and will, therefore, be described here only briefly: The test chamber and its pump consisted of two 10-in. cryogenic pumps, connected head-on by a 6-in. gate valve. After rough pumping the chamber to 10^{-4} Torr by a sorption pump, the pressure in it was lowered to better than 10^{-8} Torr by the cryogenic pump. A thick 5 by 2.5 cm gold-coated copper plate was cooled cryogenically (by the chambers's cold finger) to ~19 K, and its temperature could be controlled by heating, between 19 and 250 K, within ±1 K. A stream of water vapor, from a reservoir of thoroughly degassed triple-distilled water, was directed at the plate, through a capillary tubing with a diffuser on its tip. A ~2-μm-thick layer of ice (10^{19}—10^{20} water molecules) was deposited on the plate during 45 min. A stream of argon (Matheson Research Grade, 99.995% pure) was then directed at the ice, through the same capillary tubing, for several minutes, keeping the gate valve fully open. The flux of the impinging argon on the ice and, hence, its pressure, was obtained from the pressure drop in a vessel of a known volume and its correlation with the pressure

measured, at various plate temperatures, by the ionization gauge in the chamber. The pressure range studied was between 8×10^{-8} and 0.1 Torr.

Alternatively, a premixed argon—water-vapor mixture was flowed on the cold plate and was codeposited on it. When the deposition was terminated, the chamber was pumped for ~10 min., until a constant pressure of $\sim10^{-8}$ Torr was reached. The plate was then uniformly warmed, at a constant rate of 0.1—3 K min^{-1}. The evolution of argon and water vapor from the ice was monitored by a precalibrated quadrupole mass filter and the amounts of argon and water vapor emerging at each temperature range were obtained by integrating their fluxes over the time of their evolution from the ice.

III. RESULTS AND DISCUSSION

A. The seven ranges of gas release

The trapping and release of argon by the water ice was used to probe the ice's structure and dynamics. The trapped argon, when flowed into pure water ice or when codeposited with water vapor at ~20 K, was found to be released from the ice in seven distinct temperature ranges, starting at (a) 23 K, (b) 35 K, (c) 44 K, (d) ~80 K, (e) 136.8 K, (f) 160.0 K, and (g) ~180 K. This is in agreement with our previous findings,[1] except that the former first peak of gas evolution could now be separated into three peaks—(a), (b), and (c)—and a new, small but broad peak (d) was observed around ~80—120 K. Also, the sixth peak (f) was found now in both codeposition and when gas was flowed into the ice. As a result of these findings, the seven gas evolution ranges were relabeled from (a) to (g) in the present work, according to their increasing temperatures.

Two representative plots, showing all seven ranges of gas evolution as a function of ice temperature and of time, at a constant heating rate, are shown in Figs. 1 and 2. The first peak (a), is attributed to the evaporation of

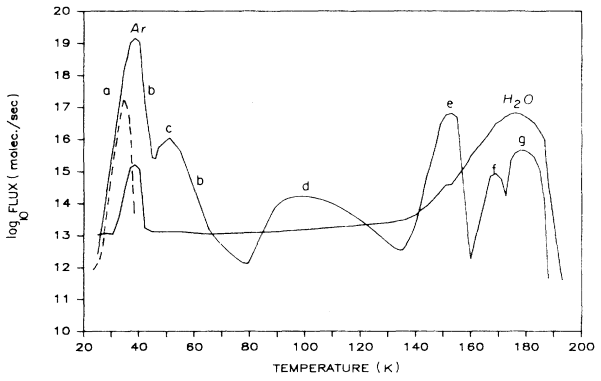

FIG. 1. A plot of the fluxes of evolved argon and water versus temperature, representing the seven ranges of gas evolution. The fluxes vary by up to 8 orders of magnitude as the ice temperature varies. Note the rise in the water flux at 30 K and at 150 K. An evaporation curve of frozen argon from an ice-free plate (— — —) is added, for comparison with the width of peak (a).

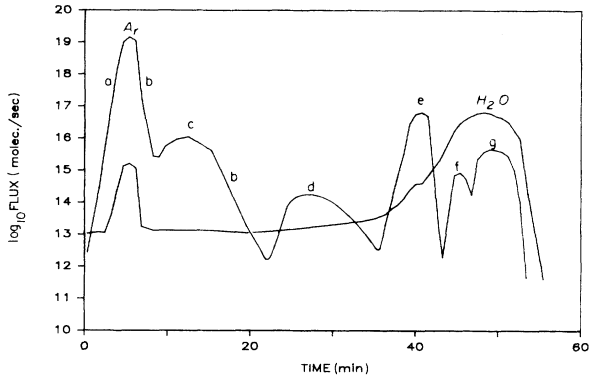

FIG. 2. A plot of the fluxes of evolved argon and water versus time. The amounts of argon and water in each peak were calculated by integrating the area under the curve.

frozen argon from the ice surface, because the temperature of the onset of evaporation and the rise in vapor pressure with temperature are identical to those of argon which was frozen on an ice-free plate. However, the decrease in the argon flux does not follow that of pure frozen argon, but extends to higher temperatures (Fig. 1). Moreover, in codeposition, or when the pressure of the flowing gas into the ice exceeds $\sim3\times10^{-4}$ Torr, gas continues to evolve from the ice at 35—60 K for tends and up to hundreds of minutes, depending upon its quantity, until it is exhausted at ~60 K. Then, its flux decreases by several orders of magnitude, to the limit of detection, 10^{10} molecule/cm^{-2}sec^{-1}. As will be shown later, the gas emerging in range (b) comes from closed holes in the ice, from which it is liberated by the slow annealing of the ice, starting at 35 K.

Following peak (a), superimposed on range (b) and resolved from them only when the amount of argon is not too large, the third peak (c) begins. Its location at a slightly higher temperature and hence higher binding energy than (a), suggests that this peak is due to the evaporation of a monolayer of adsorbed argon on the ice surface. Thus, the surface area of the ice can be determined from the amount of argon in this peak.

The small but broad peak (d), starting at ~80 K and extending up to ~120 K, was noticed only recently and has not yet been studied in detail. Gas evolution in this range depends upon the ice temperature; At a constant temperature, gas evolution declines slowly until it ceases altogether, to be resumed only when the temperature is increased by a few degrees. It seems that this range, like range (b), is related to the slow annealing of the ice.

At a temperature of 136.8 ± 1.6 K, there begins another surge of gas (e), which increases even when the ice temperature is maintained at this value, indicating a continuous change in the ice. This change is the transformation of the amorphous ice (which is formed when the ice is deposited from the vapor at a low temperature) into cubic ice. This transformation is exothermic (~90 J g^{-1}) and self-sustained.[2] The creeping of water molecules in the ice, while forming the cubic lattice, frees some of the trapped argon and squeezes it out. The onset of the transformation at 136.8 ± 1.6 K, as manifested by the on-

set of gas release, does not depend upon the heating rate between 0.1 and 3 K min^{-1}, the gas content of the ice, the amount of ice, or the rate of its deposition. This temperature is identical to the one reported by Sugisaki *et al.*[6] and close to several other reported values—133 K (Refs. 7 and 8) and 138.8 K (Ref. 9)—but disagrees with several others: 153 K,[2] 158 K,[4] 149 K,[10] and 130 K,[11] and some of the values quoted by Hobbs.[12] However, when the ice is deposited at 50—75 K, the transformation begins at 140 K, rather than 136.8 K. It seems that because of its high sensitivity, this method enables an accurate determination of the onset of the transformation. A very small peak (an argon flux of 10^{13}—10^{14} atoms cm^{-2} sec^{-1}), occurring at 125—132 K, might be interpreted as the glass transition which was found by Sugisaki *et al.*[6] The glass transition observed by McMillan and Los[10] at 139 K, occurred above the presently found transformation temperature of 136.8 K. Surprisingly, McFarlane and Angell[4] did not observe any change in the ice from 110 until 158 K, at which temperature the ice was transformed to the presumably cubic form. Perhaps their ice samples were inadvertently warmed to above 136.8 K during their transfer to the differential scanning calorimeter, and only the transformation to hexagonal ice, at 158—159 K, was measured by them.

Once the transformation to cubic ice is completed, the flow of gas from the ice decreases by several orders of magnitude, until a temperature of 160.0 ± 1.0 K is reached, where a new surge of gas begins (f). The sixth peak (f) was not always present, depending upon the deposition conditions, and sometimes it merged with the seventh peak. This gas release can be associated with the transformation of the cubic ice into hexagonal ice, which is reported to occur around this temperature, again, with a large scatter of the reported values.[12] It seems that trapped argon, which could not escape during the transformation of amorphous ice to cubic ice, finds its way out during the transformation of cubic to hexagonal ice. Here, again, the high sensitivity of gas release enables an accurate determination of the onset of the transformation: 160.0 ± 1.0 K. This value is identical to the value reported by Sugisaki *et al.*,[6] but somewhat lower than several other reported temperatures, e.g., 168.3 K (Ref. 9) and 169.5 K (Ref. 8). The very close agreement between the temperatures found in this study and those found by Sugisaki *et al.*[6] for the onset of the transformations into cubic and hexagonal ice, suggests that the vapor deposition methods used by both of us were identical, and raises the question as to what are the effects of the deposition method and further handling procedures on the amorphous ice samples.

The seventh peak of gas release (g), when well separated from the sixth peak, had its maximum 3.8 K higher than the maximum in the water evaporation peak (Fig. 1). Its decline, however, was always parallel to the decline in the water peak. This decline shows that some argon is held so tightly in the ice that it cannot escape until the ice itself evaporates. The fact that CO_2 was the only gas among those tested in our previous study which did not form this peak, and indeed should not form a clathrate-hydrate under the experimental pressure and temperature conditions,[13,14] suggested that peak (g) is due to the formation of a clathrate-hydrate. If so, then the observation of the same peak with carbon monoxide, as reported in our previous paper,[1] demonstrates the formation of a clathrate-hydrate of carbon monoxide, an abundant species in cometary comae, cometary outbursts, and dense interstellar clouds. As will be shown later, up to $\frac{1}{4}$ of the ice forms a clathrate-hydrate with argon, while the other $\frac{3}{4}$ remains as regular ice.

B. Water evaporation

As for the water ice itself, evaporation at a rate above our limit of detection (10^{10} molecule cm^{-2} sec^{-1}) is observed already at $\sim$110 K. From the increase in water flux with temperature, the heat of vaporization of the ice between 160 and 180 K was found to be $2.6\pm0.2\times10^{10}$ erg g^{-1}, in good agreement with the value of 2.79×10^{10} erg g^{-1} for pure water ice, which was calculated at 176 K, from the Clausius-Clapeyron equation and the temperature-dependent vapor pressure of water.[15] The similarity between the evaporation curves of pure ice and the clathrate-hydrate, shows that the heats of evaporation of the two are similar.

However, even well below 110 K, there is a considerable flux of water vapor when gas is emitted from the ice. Already at 30 K, where the first peak of gas emission becomes large enough, the flux of water vapor starts rising (Fig. 1), and is always 3.5—4 orders of magnitude smaller than the flux of the gas. Another increase in the flux of water vapor above that of pure ice is observed around 150 K, at the height of gas emission in range (e) (Fig. 1). The increase is by a factor of 2, regardless of the flux of the emitted gas. At 160 K, where the sixth peak (f) begins to rise, the flux of water vapor was identical to that of gas-free water ice. Thus, the heat of vaporization of water ice, which was measured between 160 and 180 K, was not affected by the presence of gas in the ice.

Apparently, when gas is flowing out of the ice, it carriers with it some loosely bound water molecules. At 30 K it takes a flow of $\sim$4000 argon atoms to release one water molecule from the very cold and rigid ice matrix, whereas at 150 K, during the transformation of the amorphous ice into the cubic form, the water molecules are more mobile and are carried away more readily by the flowing argon. Between 160 and 180 K, the flux of water molecules from the ice is so large, that an additional flux caused by the outflowing argon cannot be detected.

C. Grain ejection and argon jets

When gas is codeposited with water vapor or when gas at a pressure exceeding 2×10^{-3} Torr is flowed into the ice, ice grains are ejected along with jets of argon at the onset of range (b) and continue during gas emission in all ranges except (d) and (e) (Fig. 3). The popping of grains continues at a constant temperature for up to 6 h, becoming gradually less frequent. But, when the temperature is increased by a few degrees, the large flux of gas, grains, and jets is resumed, until all the argon in the pertinent peak is exhausted. The flux of ice grains is not always the same as that of the argon jets and, in range (d), only argon

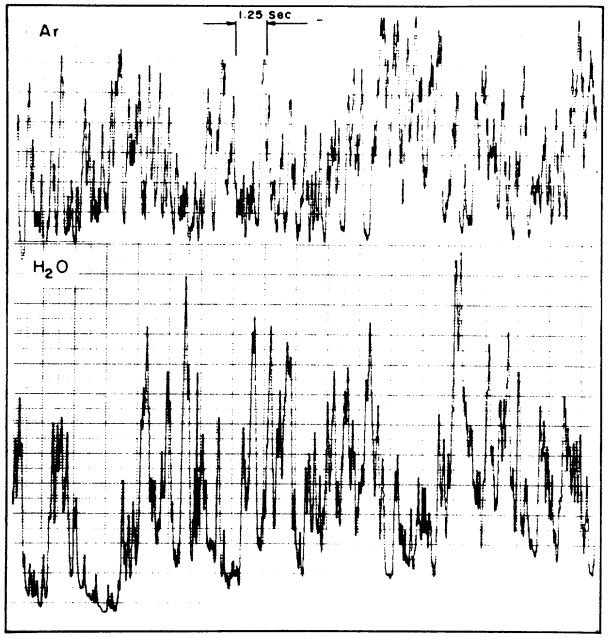

FIG. 3. Ice grains and argon jets, recorded at the same quadrupole mass-filter sensitivity.

jets are seen without any ice grains. Therefore, the argon spikes seen in the quadrupole mass filter are due partly to genuine jets of argon and partly to argon which is trapped in the ice and is released from it when the ice grains evaporate in the mass filter. In codeposition, grains and jets are emitted already when the ratio of argon in (b)—(g) to water is 0.01. Their frequency increases with the amount of argon and becomes catastrophic when this ratio reaches a value of 3.3.

A preliminary analysis of the grains which reach the quadrupole mass filter at all temperature ranges, yields radii between $\sim 0.1-1$ μm, with more in the smaller size range. Yet, in ranges (f) and (g), where the ice evaporates, grains as large as ~ 0.1 mm are seen to fall off the ice surface. The trajectories of the $0.1-1$ μm grains reaching the quadrupole mass filter imply grain speeds above 167 cm sec^{-1}. With a grain mass of 10^{-12} g, the energy propelling it should be 2.8×10^{-8} erg. The argon jets, each consisting of $\sim 10^9$ argon atoms with an average energy of kT for each atom have, already at 35 K, 200 times more energy to propel the $0.1-1$ μm ice grains at the required speed. It seems, therefore, that the argon which is trapped in closed cavities underneath the ice surface builds up enough pressure to rupture the overlying ice and propel its fragments as ice grains. This process takes place throughout the 2-μm-thick ice layer, as some holes are seen to be formed in the ice down to the plate. Even when the 2-μm-thick gas-laden ice layer is covered by a 2-μm-thick layer of gas-free ice, the rate of grain ejection is not diminished. In this case, plates of ice a few mm wide were seen to open like petals of a flower, and finally to fall off the ice. The effect of thicker ice layers was not studied yet. The picture of rupture of the ice and propulsion of its fragments is consistent with the observation that the uniform ice layer at the end of the deposition always cracks heavily at the onset of gas emission, at ~ 23 K, both in codeposition and in gas flowed into ice.

D. Gas distribution among the seven trapping mechanisms

The distribution of gas among the seven trapping mechanisms was studied in detail, over 7 orders of magnitude of the ratio of the total amount of trapped argon [in (a)—(g)] to water (R), between 10^{-4} and 10^{+3}, at 22—25 K. In Fig. 4 are shown the amounts of argon trapped in range (a), which vary by several orders of magnitude. The very sharp drop at low R shows that only the surplus gas, remaining after the other mechanisms trap their share of the gas, is frozen on the surface. Also, the curve for codeposition is much lower than that for gas flowed into ice, showing that in codeposition much more gas is trapped by the internal mechanism, as can be expected. At high R, starting at ~ 1, there is so much surplus gas that almost all of it is frozen. Also shown in Fig. 4 are the amounts of argon adsorbed as a monolayer on the ice surface (c), when flowed into it at a pressure below 10^{-5} Torr. A limiting value of argon to water equal to 0.018 is reached for the monolayer, from which the surface area of the ice can be calculated. The amounts of gas released in range (b) after flowing gas into the ice depend upon the gas pressure. At a gas pressure of 1.5×10^{-4} Torr, the argon to water ratio is 0.08, whereas at a gas pressure of 2×10^{-3} Torr, the ratio increases dramatically to 3.3. Here, the amount of argon buried in the ice is 3.3 times larger than the amount of ice itself. In codeposition, the argon to water ratios in (b) are between 0.5 and 3.5. The trapping mechanism responsible for this range will be discussed in detail later.

Figure 5(a) presents the distribution of gas among the three other internal trapping mechanisms (e), (f), and (g), with argon flowed into the ice. The amount of trapped gas increases with increasing R, until the limiting values

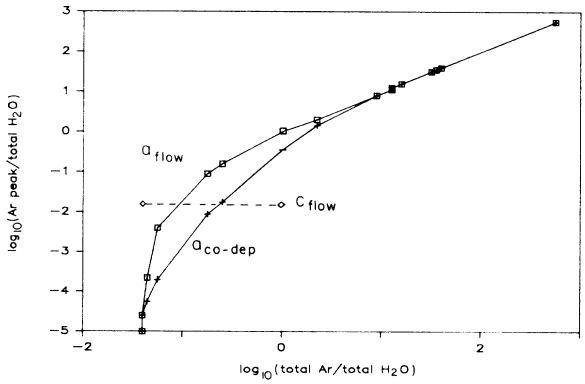

FIG. 4. The amounts of argon in range (a), for gas made to flow into ice (□) and for codeposition of a 1:1 mixture (+). Also shown are two points for range (c). Note the sharp decrease in codeposition at small total amounts of argon, as compared with the amount when argon is flowed into the ice.

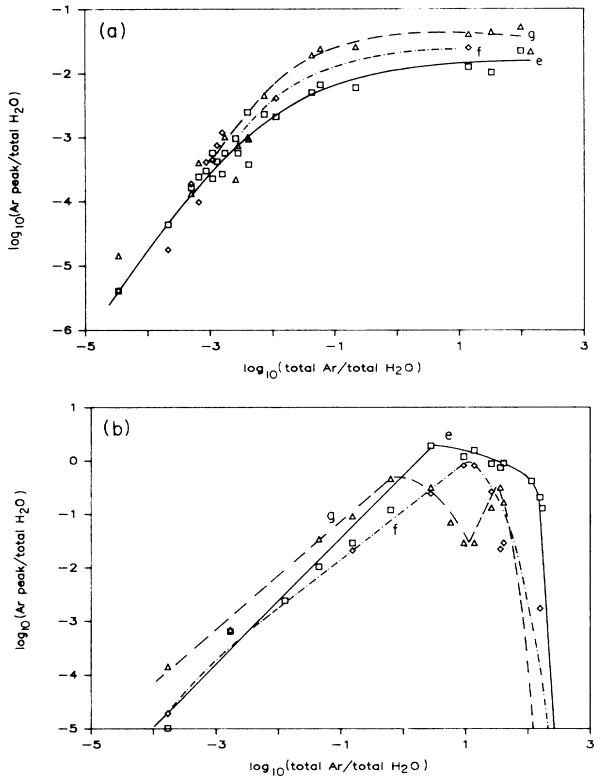

FIG. 5. The distribution of argon in ranges (e) □, (f) ◇, and (g) △, versus the total argon to total water ratio R. (a) Argon flowed into ice. Note the leveling off in all three ranges. (b) Codeposition of a 1:1 argon-water mixture. Note the lowering in range (g) at $\log_{10}(R)=0$ and its rise at $\log_{10}(R)>1$ and, also, the sharp decline of all three ranges at $\log_{10}(R)>1.5$.

of argon to water equal to 0.01, 0.015, and 0.04 are reached for (e), (f), and (g), respectively. These values are not surpassed even when the total amount of argon is increased by 3 orders of magnitude. Apparently, specific holes in the ice are involved and these are completely filled up. Argon forms a type-II clathrate-hydrate.[16] Since both small and large cages are supposed to be filled with argon atoms, an argon to water ratio of 0.17 should be reached in (g).[16] Therefore, the limiting value of 0.04 implies that only a quarter of the ice forms the clathrate-hydrate, the rest being ordinary ice.

Since peak (d) was noticed only recently, the variation of its content with R was not studied in detail. Nevertheless, it always amounts to a few percent of peak (e).

With codeposition of argon together with water vapor [Fig. 5(b)] the trapping of gas by the internal mechanisms is more efficient than by flowing gas into the ice, as can be expected. Whereas at low R the amounts of argon in (e)—(g) follow the same curve as those obtained by flowing gas into ice, they continue to increase where the others level off [Fig. 5(b)], reaching argon to water ratios of 2, 0.8, and 0.45 for (e), (f), and (g), respectively. They drop at higher R and become negligible around 200, where a loose agglomerate of ice crystals is embedded in a matrix of frozen argon and cannot hold large amounts of gas anymore. It is important to note that although the amounts of gas trapped in (e)—(g) by codeposition exceed by up to 2 orders of magnitude those trapped by flowing gas into the ice, still all the gas comes out only in these three peaks and not before or between them. Therefore, the nature of the traps is the same in the two deposition methods.

When peak (g) is small, it is symmetrical with the water evaporation curve (Fig. 1); when it exceeds the limit of 0.04, it broadens toward higher temperatures. In these cases, the ice evaporating last has an argon to water ratio of ~ 1. This behavior, which occurs only in codeposition, is understandable in view of our explanation for peaks (e) and (f): In these two peaks, the trapped gas is liberated during the transformation of amorphous ice to cubic and then to hexagonal ice. The clathrate-hydrate itself does not transform into any other crystal form until its evaporation. Hence, any excess gas which is trapped among its crystals can escape only during the evaporation of the clathrate-hydrate itself, and an argon to water ratio far in excess of the clathrate-hydrate limit of 0.17 can be reached. This finding could be of importance in the interpretation of observations of cometary phenomena. The R value where peak (g) begins to decrease [Fig. 5(b)] coincides with the onset of massive grain ejection, and the argon to water ratio reaches the bottom (0.04) where the flux of ice grains is at its peak ($R=10$). The rise which follows coincides with the slowing down of grain ejection. Apparently, when the excess gas is freed by grain ejection, the remaining ice has the same argon to water ratio (0.04) as the limit obtained by flowing gas into it. With even larger R values (>10), the ice crystals are highly dispersed in a matrix of frozen argon, which can escape more freely without rupturing the ice, and grain ejection slows down. However, a small amount of excess gas is still retained among the ice crystals and causes the rise in peak (g).

E. Ice dynamics

Trapping of large amounts of gas in water ice, by codepositing the gas together with water vapor, is more easily understood than its trapping by exactly the same seven mechanisms when flowed into preexisting amorphous ice. In order to obtain some insight into the dynamics of the process, we studied in detail the effect of temperature on the amounts of trapped gas, with special emphasis on gas flowing into ice.

Water vapor was deposited on the plate at temperatures between 19 and 80 K. Alternatively, the ice was formed on the plate at ~ 20 K and then heated to the desired temperature, where it was kept for some time. The ice was then cooled down to 22—25 K or maintained at the high temperature, and argon was flowed into it. In codeposition studies, the argon—water-vapor mixture was deposited on the plate at the desired temperature. Figure 6 shows the effect of temperature on the combined argon to water ratios in peaks (e)—(g) together. The amount of internally trapped argon drops by 4 orders of magnitude between 25 and 80 K. The decrease is the same whether the hot ice was cooled down before flowing the gas into it,

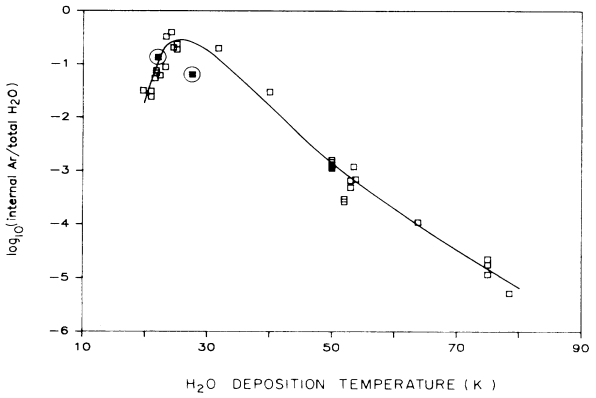

FIG. 6. The distribution of the combined amounts of argon in ranges (e), (f) and (g) versus the ice deposition temperature, for gas flowed into ice. Note the sharp decline at $T<25$ K. The circled points are those which were annealed for 5 h.

or was kept at the high temperature when the gas was introduced. Thus, the determining factor is the highest temperature at which the ice was maintained, and not its temperature during gas flow. However, the most interesting finding was that below 25 K, as the temperature drops toward 19 K, the amount of internally trapped argon decrease very sharply. The possible explanation to this behavior also explains the way in which preexisting ice traps the gas flowed into it, and does not release it until temperature of ~ 80, 136.8, and 160.0 K are reached, or until the ice itself evaporates: The amorphous ice, which is formed by depositing water vapor around 20 K, is extremely porous. Our preliminary results, using interference rings to measure the thickness of the ice layer, together with the known amount of ice, suggest a density of ~ 0.65 g cm^{-3}, as compared with 0.81 ± 0.2 g cm^{-3} at 82—85 K (Ref. 17) and 0.9 g cm^{-3} for cubic ice. Its surface area was calculated from the monolayer of adsorbed argon in peak (c), which had an average argon/water ratio of 1.78×10^{-2} (Fig. 4). The effective cross section of argon, for adsorption, is 14.6 Å^2.[18] Thus, the surface area of ice at the onset of peak (c), i.e., 44 K, was found to be 86 m^2 g^{-1}. The surface area decreases to 78, 55, and 38 m^2 g^{-1} at 75, 100, and 120 K, respectively. Mayer and Pletzer[19] found, by N_2 absorption measurements, a surface area of 43—84 m^2 g^{-1} at 77 K and a decrease to 40 m^2 g^{-1} at 113 K. However, when open micropores were added by them to the "surface area," values of high as 352—421 m^2 g^{-1} were obtained, as compared with 241 m^2 g^{-1} which was found by Ghormley.[2] These micropores disappeared altogether at 113 K. When we use the argon trapped at a pressure of 1.5×10^{-6} Torr in range (b), to calculate this so-called surface area, values of 400—500, 300—580, and 150 m^2 g^{-1} are obtained at 22, 50, and 150 K, respectively. Although the term "surface area" for trapping of gas in these micropores is misleading, it nevertheless demonstrates the extremely high porosity of the ice. The temperatures at which the surface area was found to decrease considerably are still well below the temperature of transformation of amorphous ice into cubic ice (136.8 K). It seems, therefore, that the extremely porous amorphous ice anneals even at low temperatures, and the creeping of water molecules close some of the holes in the ice. This annealing can be followed visually: The ice is heavily cracked at temperatures between ~ 20—40 K, but all the tracks disappear within a few minutes around 45 K. This is still 90 K below the temperature at which the amorphous ice transforms into its cubic form. Ghormly[20] reported that in the whole temperature range between 20 and 153 K (the onset of the transformation in his study), heat is generated in the ice by its slow annealing. Thus, the number and size of the holes in the amorphous ice diminish as its temperature increases.

When argon is flowed into the ice for a few minutes, it fills all the holes which are open to the surface. During this process, the ice creeps slowly and closes a fraction of the holes, thus trapping the argon inside the closed holes. The rate of creeping of the ice diminishes as the temperature decreases, becoming very slow below 25 K. Between 25 and 19 K, many holes remain open throughout the flow of gas and less gas is trapped inside the ice. Hence, the sharp decrease in the ratio of the internally trapped argon to water below 25 K (Fig. 6). This proposed mechanism was tested experimentally, by allowing ice samples to stay at 21 and 27 K for 5 h before flowing gas over them. The internally trapped argon to water ratio rose with the 21-K sample, which lies on the left of the maximum in the curve, whereas the ratios in the 27-K sample, which lies on the right of the maximum, decreased. These two samples are circled in Fig. 6. The increased mobility of the ice above 25 K was clearly demonstrated by Greenberg *et al.*[21] In their experiments, a frozen mixture of H_2O, CO, CH_4, and NH_3 at 10 K was irradiated in the far uv, and free radicals were formed in the rigid ice. Upon warming, at 27 K, the ice became mobile enough for the radicals to move and recombine with each other. The fast release of energy resulted in the explosion of the whole ice matrix.

Thus, the gas is trapped in slowly closing holes, during the flow of gas into the ice. A typical size of a hole can be calculated from the $\sim 10^9$ argon atoms in the argon jets, which were obtained during grain ejection. If a spherical hole is completely filled with frozen argon, whose density is 1.6 g cm^{-2},[15] the hole radius should be ~ 0.2 μm.

Once the ice is slowly warmed up, the argon which was frozen in open holes evaporates in peak (a). The increased rate of annealing of the ice in this range, at 23—35 K, closes even more gas-filled holes. At 35 K, the onest of massive grain ejections, the rate of hole closing is very fast and the built-up pressure inside the holes is large enough to rupture some of the ice and propel the fragments as ice grains. Since the ejection of ice grains is always accompanied by a continuous flux of argon, which is liberated quiescently, apparently some of the closed holes are reopened by the annealing ice. Therefore, with smaller amounts of argon, the ice is not ruptured and the gas is liberated slowly in (b), by the slowly annealing ice. By the time gas emission in range (a)—(c) is completed, the ice went through many minutes at 45—55 K where the creeping is visually very fast and the holes are closed even more

tightly. Further annealing seems to be responsible for the broad peak (d), which starts at ~80 K and continues until ~120 K. The process which liberates the gas in this range is temperature dependent since, at a constant temperature, gas evolution declines slowly until it ceases altogether after tens of minutes, to be resumed only when the temperature is increased by a few degrees. The evolution of heat between 20—153 K, as reported by Ghormly,[20] is another manifestation of the annealing, although he did not describe any particular behavior between ~80—120 K. The gas which was not liberated in (a)—(d) is completely locked in the ice, until it is transformed into cubic ice. During this fast and exothermic transformation, the ice matrix becomes temporarily loose, letting out a fraction of the trapped argon. However, the very mechanism which frees some of the gas compacts the ice in its cubic form and traps the remaining gas even more tightly. The liberation of this gas is delayed until the next transformation from cubic to hexagonal ice.

The question then arises as to at what stage is the clathrate-hydrate formed? Below 25 K, as shown above, the mobility of the water molecules is so small that it seems rather unlikely that they would move from their sites in the amorphous ice to form the cages of the clathrate-hydrate. Rather, the clathrate-hydrate seems to be formed around the closed holes which contain the argon, when the temperature increases and the water molecules become more mobile probably around 35—45 K, where the annealing is visually very fast. The limit of a quarter of the ice forming a clathrate-hydrate could not be surpassed, even in the presence of a huge amount of argon. This has to do with the impermeability to gas molecules of the clathrate-hydrate lattice, which was formed on the walls of the gas-filled cavities. Thus, once a layer of a clathrate-hydrate forms, it prevents further contact between gas atoms in the cavity and the rest of the ice. Indeed, in studies where all the ice has to be transformed into a clathrate-hydrate, the ice is constantly crushed by glass or steel balls.[22,23]

In codeposition, the amorphous ice is formed in the presence of plenty of argon and, obviously, larger and more numerous gas-filled holes can be formed and close under additional layers of ice. Therefore, at the same temperatures and pressures, the amount of trapped gas in all the five internal traps is 25—1500 times larger than when gas if flowed into ice.

The effect of argon pressure, during its flow into the amorphous ice, was also studied. The gas pressure was varied between 8×10^{-8} and 3×10^{-4} Torr at 25, 40, 50, and 75 K. All three peaks, (e), (f), and (g), behaved in a similar manner and are therefore lumped together in Fig. 7. As can be seen in the figure, a higher gas pressure can compensate to some extent for an increase in temperature, by compressing more gas into the open holes, or by forcing its way into other holes. Thus, at 50 and 75 K, an increase in pressure by 4 orders of magnitude increases the amount of trapped argon by 1.5 orders of magnitude. But at 25 K, where the internal traps are almost completely filled, the effect of pressure is smaller. A few points of codeposition are also added to Fig. 7, to demonstrate the sharp increase in the amount trapped by this method.

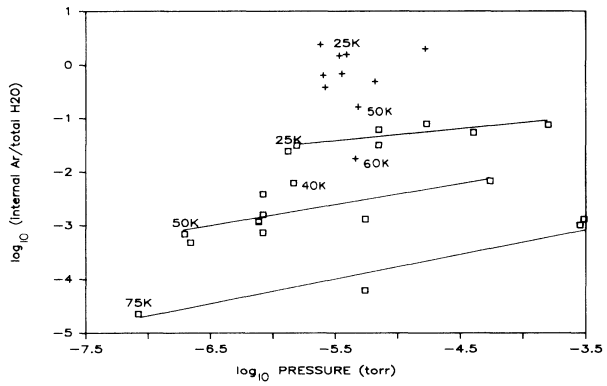

FIG. 7. The effect of gas pressure and temperature, during gas flow into ice, on the combined amount of argon in ranges (e), (f), and (g). Some points from codeposition of a 1:1 argon-water vapor mixture are added, for comparison (+).

The effect of pressure is most dramatic in range (b): Up to a gas pressure of 2×10^{-3} Torr (2.6 dyn cm^{-2}) the gas content in range (b) rises gradually with increasing pressure. However, at and above this pressure, the gas content suddenly becomes huge, 3.3 times larger than the amount of the ice itself. This amount is identical to the highest obtainable by codeposition. Another similarity is the large rate of grain ejection and argon jets, observed in both cases. It seems, therefore, that by flowing argon at 2×10^{-3} Torr into amorphous ice, its trapping becomes identical to that of codeposition. In order to trap such huge amounts of argon in the preexisting amorphous ice, the gas has to penetrate into deep underlying layers by breaking the ice matrix.

The density of the water ice matrix, which holds the frozen argon, can be calculated from the relative amounts, by number, of the water ($n\mathrm{H_2O}$) and the argon which is held in the internal traps (nAr): The density of compact ice is 0.9 g cm^{-3} and that of frozen argon 1.6 g cm^{-3}. Their respective molecular weights are 18 and 40. N is Avogadro's number and $r=n\mathrm{Ar}/n\mathrm{H_2O}$. When completely filled with frozen argon, the ice-argon matrix occupies a volume V, where

$$V=18n\mathrm{H_2O}/0.9N+40n\mathrm{Ar}/1.6N\ .$$

If all the internally trapped argon is removed, a fluffy ice matrix is left behind, whose density is

$$\rho=(18n\mathrm{H_2O}/N)/(18n\mathrm{H_2O}/0.9N+40n\mathrm{Ar}/1.6N)$$
$$=1.8/(20+25r)\ .$$

In the case of argon flowed into ice at a pressure of 2×10^{-3} Torr, which was described above, $r=3.3$ and $\rho=0.18$ g cm^{-3}. This density for ice is extremely low, and suggests that the ice matrix is like a fluffy foam. A similar ice matrix is obtained by codeposition: From Fig. 5(b), the combined amounts of argon in the internal traps (excluding the clathrate-hydrate) give at their maximum (at $R=20$), $r=3.5$ and $\rho=0.17$ g cm^{-3}. At higher values

of R, as mentioned earlier, the ice matrix collapses altogether. It seems, therefore, that $\rho=0.17$ g cm^{-3} represents the maximum porosity of the ice matrix, which still retains its structure, and this very fluffy porous amorphous ice is formed by both codeposition and by flowing gas at a pressure above 2×10^{-3} Torr into the ice.

IV. CONCLUSIONS

The picture of the amorphous ice, which emerges from this study, is that of a highly porous matrix, with a density of ~0.65 g cm^{-3} and a surface area of ~90 m^2 g^{-1}, at 44 K. The porous matrix anneals at all temperatures, closing and reopening holes in the ice at a rate which is strongly temperature dependent. At 136.8 ± 1.6 K the amorphous ice transforms into cubic ice, which turns into hexagonal ice at 160.0 ± 1.0 K. During both transformations, the ice becomes temporarily more mobile.

The very high porosity of the amorphous ice allows large amounts of gas to settle in the vast number of cracks and open holes. Once these are filled and a monolayer of adsorbed gas is formed, the surplus gas freezes on the ice's surface. The single process which locks the gas in the ice is the temperature-dependent creeping of the ice. During the flow of gas into the porous ice and also during the evaporation of the frozen gas (a) from 20 to 35 K the ice creeps and closes many gas-filled holes and cracks. The continuous creeping of the ice (visible at ~45 K) reopens some of the holes and liberates some trapped gas from 35 up to ~60 K (b) and, again, from ~80 to ~120 K (d). This annealing locks the rest of the gas inside a compact and impermeable ice matrix. The next chance for gas to escape occurs during the transformation of the amorphous ice to cubic ice (e), when the ice becomes temporarily more mobile. While doing so, the ice locks the rest of the gas, which can escape only during the next transformation, into hexagonal ice (f). At an early stage of the process, a clathrate-hydrate of argon is formed on the walls of the gas filled holes. The clathrate-hydrate is impermeable to the gas and stops this process when only up to $\frac{1}{4}$ of the ice is converted to the new crystal structure. When the clathrate-hydrate evaporates (g), the gas and water are released simultaneously. The heat of vaporization of the clathrate-hydrate is similar to that of pure water ice.

The very good reproducibility of the results and the smooth changes over 7 orders of magnitude in the total argon content, demonstrate the regularity of the creeping of the ice. As the amount of argon increases, each of the five internal traps (b), (d), (e), (f), and (g) gets its share of the gas, in parallel with the others, up to a limit which cannot be surpassed. The continuous annealing explains also the sharp reduction in the trapping capacity of ice which was warmed to higher temperatures.

Obviously, much larger amounts of gas can be trapped by the internal traps during codeposition than during gas flow into the ice, because of the continuous formation of overlying ice layers. In codeposition, some additional gas is trapped among the clathrate-hydrate crystals, which do not undergo any transformation until their evaporation. Thus, when the clathrate-hydrate evaporates, it releases amounts of gas in excess of the gas to water limit of the clathrate-hydrate. Altogether, the internal traps (b)—(g) can hold a quantity of gas which is 3.3 times larger then the amount of ice itself.

The amorphous ice matrix is extremely fragile. A gas pressure of only 2×10^{-3} Torr (2.6 dyn cm^{-2}) is capable of breaking its internal structure and "inflating" it to a density of merely 0.17 g cm^{-3}. The fragility of the ice is demonstrated also by the huge flux of 0.1—1 μm (and ~0.1 mm during ice evaporation) ice grains, which accompanies the release of large quantities of trapped gas. The accompanying argon jets have enough energy to propel the grains at speeds exceeding 167 cm sec^{-1}. If the holes in the ice are initially filled with frozen argon, their radii would be of the order of 0.2 μm, similar to the grain radii. Some water molecules are held so loosely in the ice, so that even during the evaporation of the frozen gas, at ~30 K, water molecules leave the ice, with a gas to water ratio of ~4000. At ~150 K, where the transformation of amorphous to cubic ice takes place, the relatively mobile water molecules leave the surface more easily, and their flux during gas escape exceeds the vapor pressure curve of the ice by a factor of 2.

The results of this study could be of importance to our understanding of the formation and behavior of icy bodies in the solar system.[24]

ACKNOWLEDGMENTS

This research was supported by the NASA Exobiology Program, through the State University of New York at Stony Brook.

[1]A. Bar-Nun, G. Herman, D. Laufer, and M. L. Rappaport, Icarus **63**, 317 (1985).
[2]J. A. Ghormly, J. Chem. Phys. **46**, 1321 (1967).
[3]C. A. Angell, Annu. Rev. Phys. Chem. **34**, 593 (1983).
[4]D. R. McFarlane and C. A. Angell, J. Phys. Chem. **88**, 759 (1984).
[5]A. Bar-Nun, G. Herman, M. L. Rappaport, and Yu. Mekler, Surf. Sci. **150**, 143 (1985).
[6]M. Sugisaki, H. Saga, and S. Seki, J. Chem. Soc. Jpn. **41**, 2591 (1968).
[7]H. Konig, Nachra. Acad. Wiss. Goettingen **1**, 1 (1942).
[8]M. Blackman and N. D. Lisgarten, Proc. R. Soc. London, Ser. A **239**, 93 (1957).
[9]H. Fernandez-Moran, Ann. N.Y. Acad. Sci. **85**, 689 (1960).
[10]J. A. McMillan and S. C. Los, Nature (London) **206**, 806 (1965).
[11]A. Defrain and N. T. Linh, C. R. Acad. Sci. **263**, 1336 (1966).
[12]P. V. Hobbs, *Ice Physics* (Clarendon, Oxford, 1974), pp. 58 and 59.
[13]S. L. Miller and W. D. Smythe, Science **170**, 531 (1970).
[14]L. A. Lebofsky, Icarus **25**, 250 (1975).
[15]*CRC Handbook of Chemistry and Physics* (CRC Press, Boca Raton, Florida, 1982).
[16]D. W. Davidson, Y. P. Handa, C. I. Ratcliff, J. S. Tse, and B.

M. Powell, Nature **311**, 142 (1984).
[17]B. A. Seiber, B. E. Wood, and A. M. Smith, Science **170**, 652 (1970).
[18]V. Ponec, Z. Knor, and S. Cerny, *Adsorption on Solids,* English translation by D. Smith and N. G. Adams (Butterworths, London, 1974), p. 542.
[19]E. Mayer and R. Pletzer, Nature **319**, 298 (1986).
[20]J. A. Ghormly, J. Chem. Phys. **48**, 503 (1968).
[21]L. B. D'Hendecourt, L. J. Allamandola, F. Baas, and J. M. Greenberg, Astron. Astrophys. **109**, L12 (1982).
[22]R. M. Barrer and D. J. Ruzicka, Trans. Faraday Soc. **58**, 2262 (1962).
[23]D. W. Davidson, in *Water: A Comprehensive Treatise,* edited by F. Frank (Plenum, New York, 1973).
[24]D. Prialnik and A. Bar-Nun, Astrophys. J. (to be published).